

Multi-wavelength study of energetic processes during solar flare occurrence

Shirsh Lata Soni^{1,2,3}, Manohar Lal Yadav², Radhe Shyam Gupta¹ and Adya Prasad Mishra³

¹ Department of Physics, Govt. P.G. College Satna MP, 485001 India; sheersh171@gmail.com

² KSKGRL, Indian Institute of Geomagnetism, Allahabad 211003, India

³ Department of Physics, Awadhesh Pratap Singh University, Rewa MP 486001, India

Received 2020 March 7; accepted 2020 April 29

Abstract This paper is an attempt to understand the physical processes occurring in different layers of the solar atmosphere during a solar flare. For a complete understanding of the flare, we must analyze multi-wavelength datasets, as emission at different wavelengths originates from different layers in the solar atmosphere. Also, flares are transient and localized events observed to occur at all longitudes. With these considerations, we have carried out multi-wavelength analysis of two representative flare events. One event occurred close to the center of the solar disk and the other occurred close to the limb. In the former case, we examine emission from the lower layers of the solar atmosphere. Therefore the chromosphere, transition region and also photospheric magnetogram can be analyzed. On the other hand, in the near-limb event, coronal features can be clearly examined. In this paper, the first event studied is the M1.1 class flare from the active region NOAA 10649 located at S10E14 and the second event is the M1.4 class flare from the active region 10713 located at S12W90. In both cases, we have acquired excellent multi-wavelength data sets. The observations from multi-instrumental data clearly demonstrate that flares occur in the vicinity of sunspots. These are regions of strong magnetic field with mixed polarity.

Key words: sun — solar flare — activity

1 INTRODUCTION

The study of multi-wavelength emission during solar flares has enormous potential towards understanding the underlying physical phenomena occurring in the solar atmosphere. It is generally accepted that magnetic reconnection is responsible for the sudden energy release and acceleration of particles in solar exploration (solar flare) (Joshi et al. 2011). In a solar flare, deviation of the magnetic field from the potential field is associated with the energy storage and release process. Therefore, researchers have studied the temporal and spatial correspondence between flare occurrence and photospheric magnetic field properties in order to characterize the magnetic non-potentiality (e.g., Hagyard et al. 1984; Hagyard 1990; Abramenko et al. 1991; Wang et al. 2007; Cui et al. 2006; Pevtsov et al. 2003; Deng et al. 2001; Moon et al. 2002; Joshi et al. 2012; Kumar et al. 2011), since the study revealed that the flare ribbons are preferentially located along the polarity inversion line (PIL) with a strong magnetic gradient and a high magnetic shear. The other important quantity considered to study and monitor the evolution of magnetic non-potentiality in a flare is electric

current. On the other hand, based on multi-wavelength study, a standard model called the CSHKP model was developed (Abramenko et al. 1991; Sturrock 1996; Hirayama 1974; Kopp & Pneuman 1976), which can explain the flare features of the separating two ribbons observed by H-alpha/ultraviolet (UV) and the expanding soft X-ray loops. In this present study, we analyze the physical process of energy release during solar flares. These solar flares occurred at different longitudes on the solar disk so here it is important to study behavior of the solar flare emission with different angles. For that, we have chosen two flares; one of them happened near the center of the solar disk at the southeast region, with heliographic coordinates S10E14 from active region NOAA 10649 on 2004 July 17 and the other is a limb event which transpired on 2004 December 29 in the active region 10713, located close to the limb of the Sun at the southwest region, with heliographic coordinates S12W90. Both flares are nearly the same class of intensity, M-class (*GOES* intensity classification). With the help of various imaging instruments onboard different satellites with multiple energy bands and time resolutions, we are trying to analyze the energy release process during

flares. The study of solar flares is exciting and challenging. The observations of solar flares provide us a wealth of knowledge about the basic plasma processes (such as magnetic reconnection) and behavior of magnetized plasma in high temperature environments. Further, understanding the behavior of solar flares enables us to study similar processes in other stars and astrophysical systems. This requires multi-wavelength observations of the Sun with high temperature and spatial resolutions. Technological developments have provided us with the capability to look further into aspects that have been invisible in the past. Future scientific research would lead to better understanding of the Sun-Earth system.

2 DATA SOURCES

The present analysis is based on data taken from the following instruments: magnetograms observed by *Solar and Heliospheric Observatory (SOHO)*/Michelson Doppler Imager (MDI); X-ray measurements from *GOES* and *Reuven Ramaty High Energy Solar Spectroscopic Imager (RHESSI)*; UV and extreme ultraviolet (EUV) images from *Transition Region and Coronal Explorer (TRACE)*. *TRACE* obtained 1 arcsec resolution, multithermal images of the solar atmosphere with a cadence and continuity of coverage commensurate with the variability and lifetimes of primary solar targets such as X-ray bright points, active regions, filaments and flares. *TRACE* records UV and EUV multilayers with different wavelength filters (2500 Å, 1700 Å, 1600 Å, 1550 Å, 1216 Å, 284 Å, 195 Å, 171 Å). For the present study, we have examined the 1600 Å filter images which image chromospheric features in the UV region and 195 Å filter images corresponding to the coronal region of the solar atmosphere and the filter is sensitive to a temperature of about 1.5 million K. *SOHO*/MDI measures line-of-sight motion (Dopplergrams), magnetic field (magnetograms) and brightness images of the full disk at several resolutions (4 arcsec to very low resolution) and a fixed selected region in higher resolution (1.2 arcsec). *GOES* X-ray sensors observe the Sun continuously in two broadband soft X-ray channels (1–8 Å) and the harder channel (0.5–4 Å) which provides information on coronal plasma. From *GOES* X-ray data we can compute the effective color temperature and emission measure for the solar flare with 3-second time resolution. *RHESSI* is designed to investigate particle acceleration and energy release in solar flares through imaging and spectroscopy of hard X-rays and gamma rays. It images solar flares in energetic photons from soft X-rays (~ 3 keV) to gamma rays (up to ~ 20 MeV) and enables high resolution spectroscopy up to gamma ray energies of ~ 20 MeV. Its rotating modulated collimators allow angular resolution down to 2.3 arcsec.

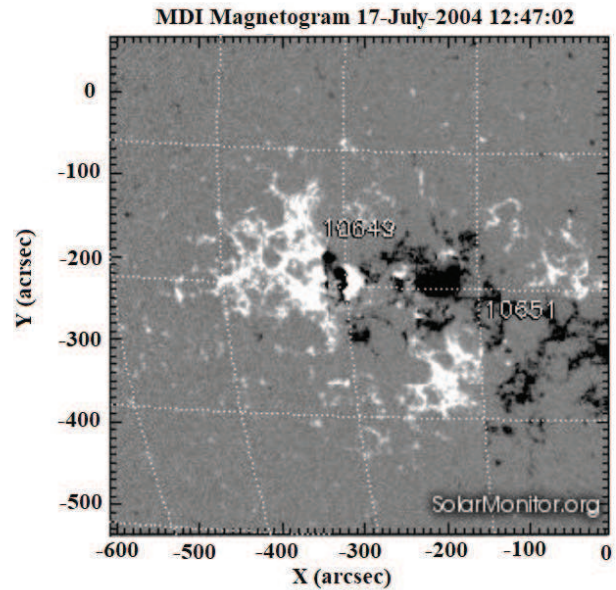


Fig. 1 *SOHO*/MDI magnetogram observed on 2004 July 17. The image displays the active region NOAA 10649.

The data analysis in this paper was performed utilizing interactive data language (IDL) programming and Solarsoft.

3 MULTI-WAVELENGTH OBSERVATIONS OF TWO M-CLASS SOLAR FLARES

The standard flare model, also known as the CSHKP model, recognizes that the evolution of flare loops and ribbons can be understood as a consequence of the relaxation of magnetic field lines stretched by the ejection of plasma (Abramenko et al. 1991; Lin et al. 2002). Magnetic reconnection has been identified as the key process which releases sufficient magnetic energy on short time scales to account for the radiative and kinetic energies observed during an eruptive event (Priest & Forbes 2002). A solar flare is a multi-wavelength phenomenon. Therefore in order to gain a complete understanding of its temporal evolution, we need to examine time profiles recorded at different wavelengths. However, it has been noted that there could be subtle activities at the flare location before its onset. In the following, we discuss different aspects of flare evolution.

3.1 M1.1 Class Flares on 2004 July 17

The MDI instrument on *SOHO* provides almost continuous observations of the Sun and records magnetograms. The first event selected for the study in this paper occurred on 2004 July 17. The flare was observed in the active region 10649, located near the center of the solar disk at the southeast region, with the heliographic coordinates S10E14. The magnetogram of the active region 10649 is

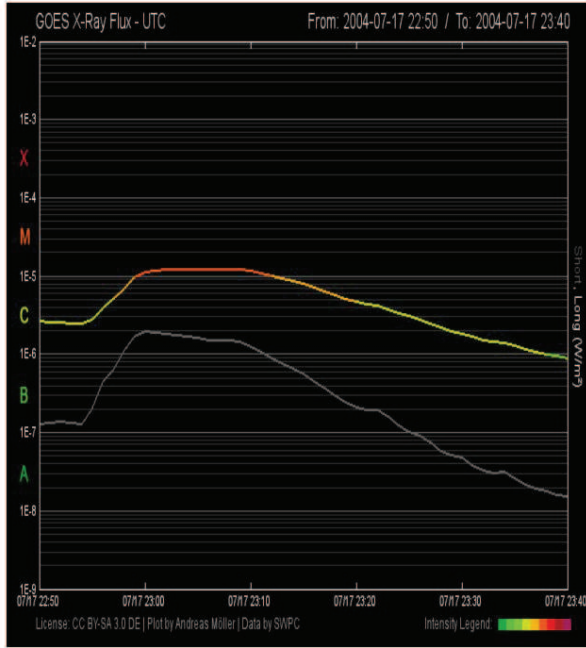


Fig. 2 Temporal evolutions of *GOES* soft X-ray for the M1.1 flare on 2004 July 17. The colored line signifies the plot in the 1.0–8.0 Å (12.5–1.5 keV) channel and the solid grey line represents the plot in the 0.5–4.0 Å (24.0–3.0 keV) channel.

depicted in Figure 1. The image clearly displays groups of sunspots as the leading active region (indicated by arrows). The image represents the magnetic field of the active region in black and white which correspond to the regions of south and north polarity, respectively. Although the leading sunspot is larger in size, it has a simplified magnetic structure. However, the following sunspot has a complex magnetic structure with mixed polarity. Figure 2 shows the *GOES* soft X-ray light curve obtained in two different channels (wavelengths 1.0–8.0 Å and 0.5–4.0 Å). The wavelength 1.0–8.0 Å corresponds to energy 12.5–1.5 keV and 0.5–4.0 Å corresponds to energy 24.0–3.0 keV. According to the *GOES* profile, the event took place between 22:54 UT and 23:20 UT, with maximum emission at 23:00 UT. It is evident that there is a gradual rise during the initial phase of the flare. It is interesting to note that there is no significant decrease in the soft X-ray flux for ~10 minutes after the peak at 23:00 UT. This feature of the soft X-ray profile is more noticeable in the 1.0–8.0 Å light curve, in which the flux is almost sustained between 23:00 UT and 23:10 UT. Then this event continues to decline gradually after ~23:10 UT. From the *GOES* flux data, it is recorded as an M1.1 class soft X-ray flare based on the peak intensity of emission. The flare was also observed by the *RHESSI* spacecraft. The *RHESSI* X-ray light curves are obtained for energy bands of 6–12 keV, 12–25 keV and 25–50 keV, as seen in Figure 3. Similar to the *GOES* pro-

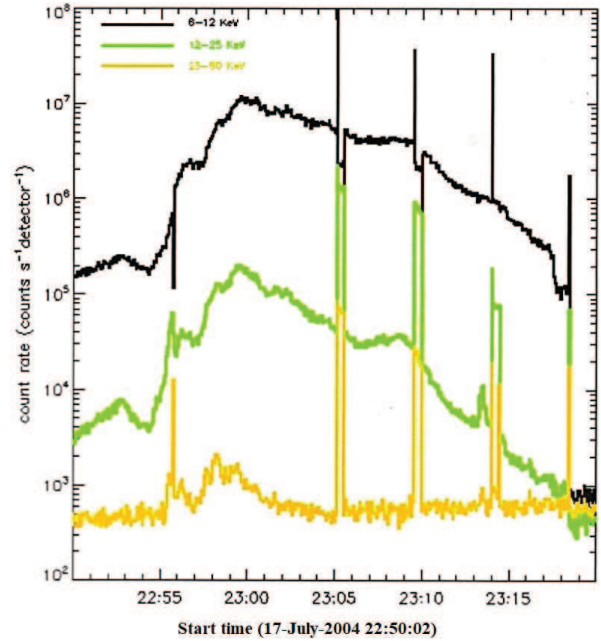


Fig. 3 Temporal evolution of X-ray plot from *RHESSI*. The *RHESSI* time profiles are obtained for energy bands of 6–12 keV, 12–25 keV and 25–50 keV. The sharp changes in the time profile are due to the instrument artifact corresponding to change in the attenuator state.

file, the rise of the initial phase is visible at ~22:54 UT in both 6–12 keV and 12–25 keV energy bands. However, the hard X-ray profile is impulsive in nature and shows a maximum intensity at ~22:58 UT. The difference in timing from the observation of the maximum phase between hard X-ray and soft X-ray (~2 minutes) is noteworthy. The flare observations were also made by the *TRACE* satellite. We have used *TRACE* 195 Å and 1600 Å wavelength filters in the EUV and UV spectral range respectively for flare observation.

The *TRACE* 195 Å images correspond to the coronal region of the solar atmosphere and the filter is sensitive to a temperature of about 1.5 million K. The observations of the M1.1 class flare in *TRACE* 195 Å have been recorded completely from the initial phase of the flare to the final phase. Figure 4 depicts the series of flare images by *TRACE* 195 Å. The images acquired during the initial phase (~22:55:20 UT) clearly demonstrate that the emission originates from two regions in the flaring location. For convenience, let us call them the eastern brightening and western brightening, respectively. These two bright regions are well separated from one another and their structures are clearly observed. The magnetic loops connecting the regions are also visible in the images. As the flare evolves, the structure of the two bright regions changes, as seen in Figure 4 at 23:00:32 UT. A little while later, these bright regions are no longer resolved well. They are connected

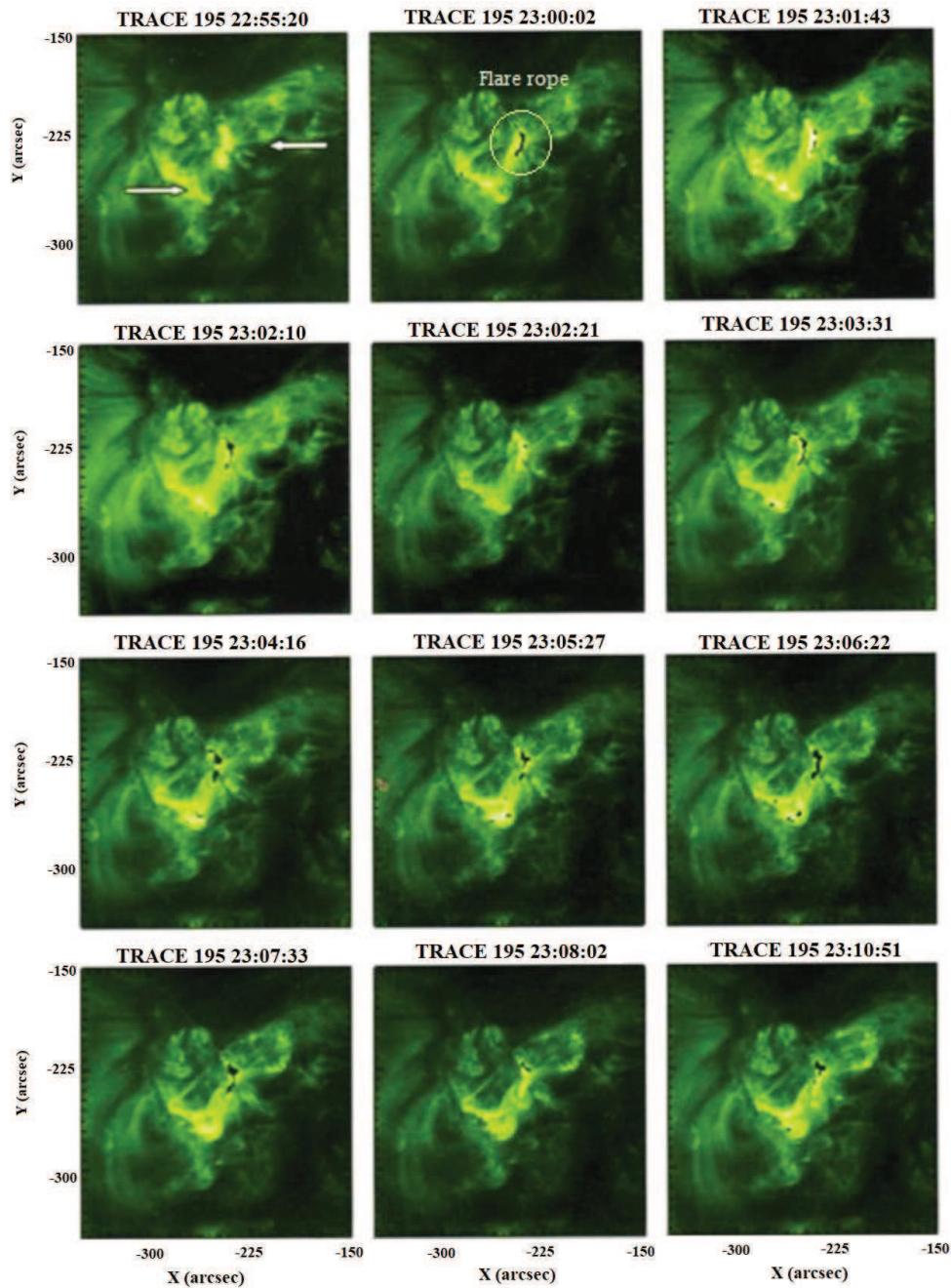


Fig. 4 Sequential *TRACE* 195 Å images of active region 10649 during the flare. The images are recorded from the initial phase (22:50:20 UT) to the decay phase (23:10:51 UT) of the flare.

to one another, and another region appears as one bright structure shaped like a V, as visible at 23:02:10 UT. This connection between the eastern and western brightenings is due to the release of high energy by the process of magnetic reconnection. As the energy is released, the plasma is heated to high temperatures and the separation between the two regions is filled by hot plasma. Further as the plasma cools, the two regions become well resolved again, as visible at 23:02:21 UT. Yet again, the energy is released and hot plasma fills the separation and cools at a later time. The

series of EUV images suggest that the process of pumping of plasma is repeated a few times until 23:10:51 UT. We interpret this process as the distinct events of energy release during the flare evolution. This process of episodic energy release is clearly reflected in the *GOES* soft X-ray light curve in the form of prolonged maximum phase. As discussed earlier, the maximum phase is observed to be sustained from 23:00 UT to 23:10 UT and the corresponding analysis of *TRACE* 195 Å between these periods provides a consistent picture with the bright fuzzy structure

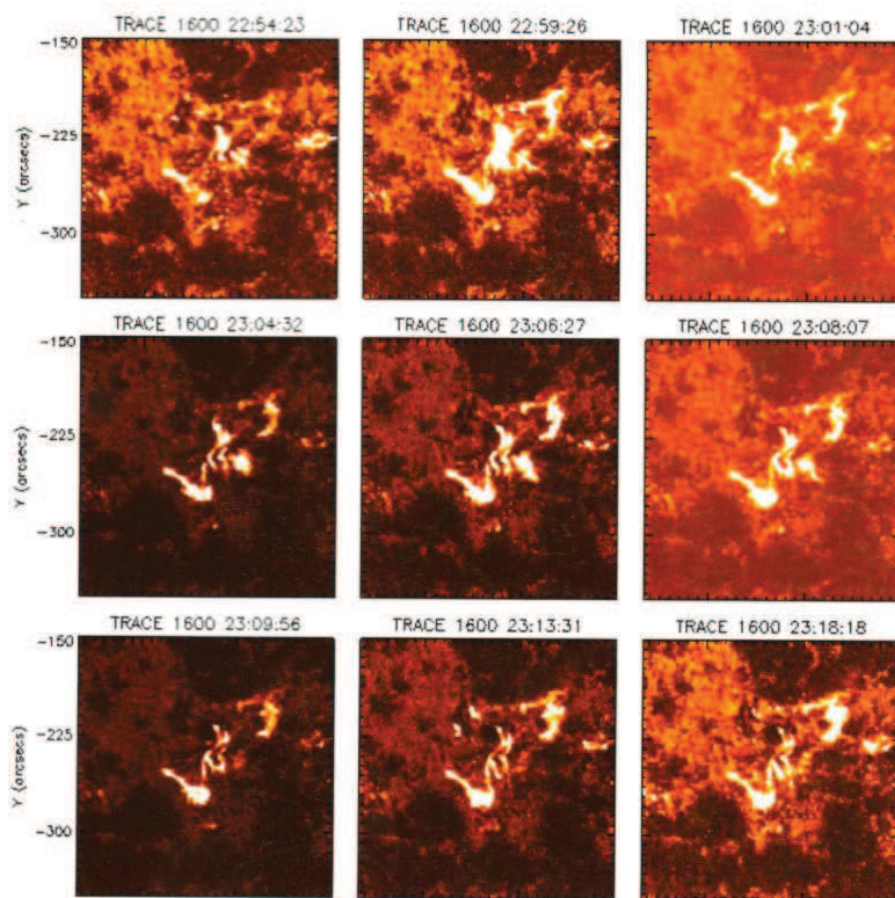


Fig. 5 Sequential *TRACE* 1600 Å images of active region 10649 during the flare. The images are recorded from the initial phase (22:54:23 UT) to the late decay phase (23:18:18 UT) of the flare.

observed in EUV *TRACE* images corresponding to plasma at very high temperature. It is also observed that at high temperature during release of energy, the plasma spreads out and is observed in a larger volume. As the temperature reduces, the structures are resolved and the hot plasma now occupies lesser volume. Throughout the flare, the eastern brightening evolves and significant change in its structure is clearly seen, due to the energy release process. Therefore, from comparison of the X-ray light curve with the EUV images, the prolonged maximum phase of the flare can be understood well.

The *TRACE* 1600 Å image corresponds to the chromospheric and transition region of the solar atmosphere and is sensitive to temperature in the range 5000–10 000 K. Observations of the M1.1 class flare in *TRACE* 1600 Å have also been recorded from the initial phase to the decay phase. The series of images of the flare from *TRACE* 1600 Å is depicted in Figure 5. The bright regions, as seen in 195 Å filter images, are also observed here. This provides evidence that during the flare there is a link in the processes occurring in the different layers of the solar atmosphere extending from the corona to the chromo-

sphere. Similar to the *TRACE* 195 Å images, two well resolved bright regions are observed. Also, several ribbon-like bright regions are electrons in the lower layers of the Sun. The electrons present in the solar corona are accelerated and distinct changes in the active region are visible until 23:13:31 UT. We observe rather small changes during the decay phase of the flare.

3.1.1 M1.4 class flare on 2004 December 29

The second flare event selected for the study in this work occurred on 2004 December 29. The flare was observed in the active region 10713, located close to the limb of the Sun at the southwest region, with heliographic coordinates S12W90. The present analysis is based on data taken from the following sources: magnetograms and intensitygrams observed by the *SOHO*/Michelson Doppler Imager; X-ray measurements from *GOES* and *RHESSI*; EUV images from *TRACE*. In Figure 6 we present the magnetogram of the active region 10713 on 2004 December 27 that represents the magnetic field strength and polarity in the Sun's photosphere. On the day the flare occurred, the region of

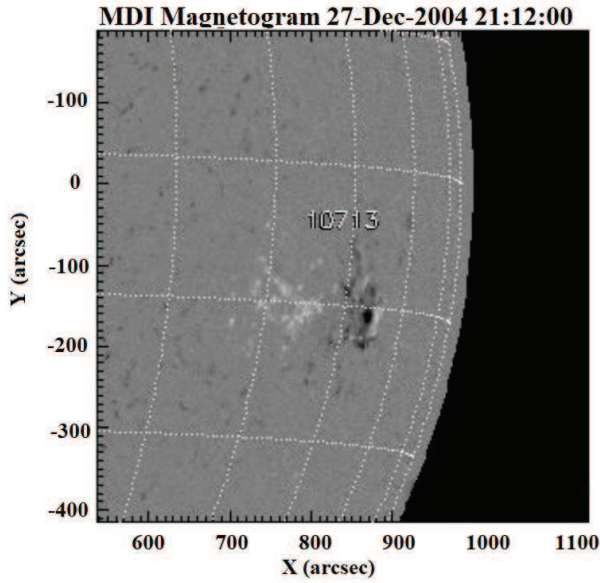


Fig. 6 *SOHO/MDI* magnetogram observed on 2004 December 27, two days prior to the event studied. The image features the active region 10713.

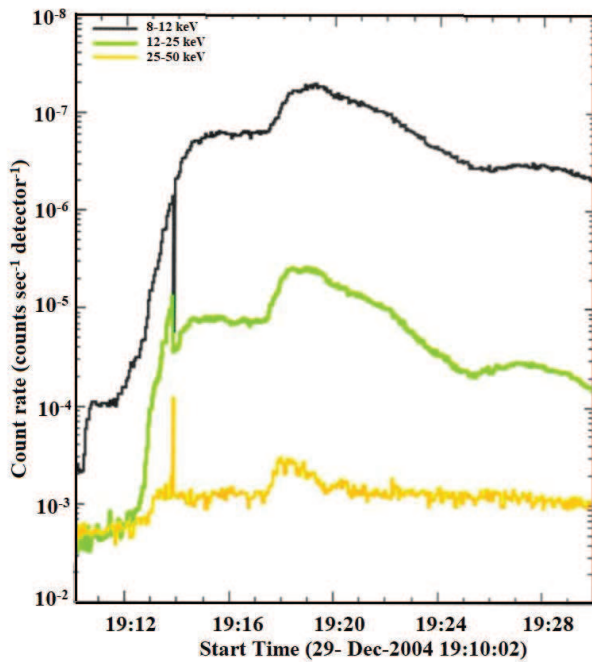


Fig. 7 Temporal evolution of *GOES* soft X-rays for the M1.4 flare on 2004 December 29. The dotted line traces the plot in the 1.0–8.0 (12.5–1.5 keV) channel while the solid line represents the plot in the 0.5–4.0 (24–30 keV) channel.

interest was located very close to the solar limb. In such situations, we hardly resolve any detailed structures due to the projection effects. Therefore, we have selected the magnetogram of the active region two days prior to the event. The image represents the magnetic field of the active

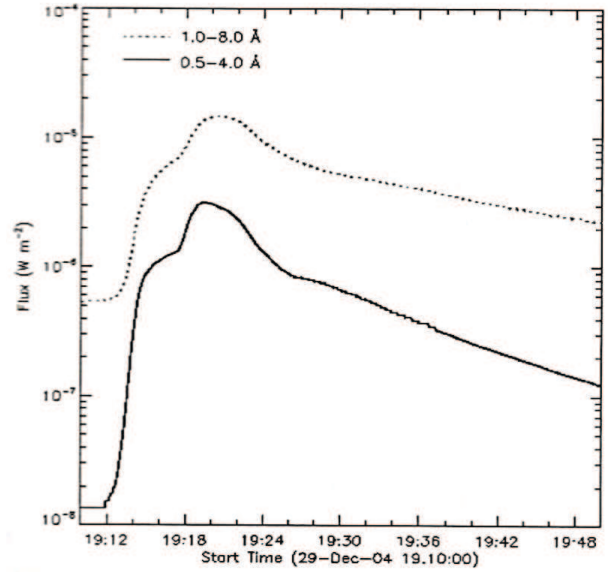


Fig. 8 Temporal evolution of X-rays plotted from *RHESSI*. The *RHESSI* time profiles are obtained for energy bands of 6–12 keV, 12–25 keV and 25–50 keV. The sharp changes in the time profile are due to the instrument artifact corresponding to change in the attenuator state.

region in black and white colors which correspond to the region of south and north polarities, respectively. Figure 7 displays the *GOES* X-ray flux light curve obtained in two different channels with wavelengths 1.0–8.0 Å and 0.5–4.0 Å respectively. According to the *GOES* light curve, the event took place between 19:12 UT and 19:40 UT with maximum emission at 19:20 UT. In the initial phase of the flare, there is a steep rise from $\sim 19:12$ UT. However, at 19:15 UT there is a change in the trend of the light curve. Again at 19:18 UT there is a sharp and fast rise. Thus, we note that the evolution of the flare takes place in two stages. After peak at $\sim 19:20$ UT, the soft X-ray flux begins to decay. We see a faster decay until 19:27 UT. Additionally, we ascertain a gradual decline in the soft X-ray flux. Hence, the flare also decays in two stages. From the *GOES* flux data, it is recorded as an M1.4 class soft X-ray flare.

The flare was also observed by the *RHESSI* spacecraft. The *RHESSI* X-ray light curves are obtained for energy bands of 6–12 keV, 12–25 keV and 25–50 keV, as visible in Figure 8. It was also found that emission was observed above the 50 keV energy band. Variations in the *RHESSI* light curves are very similar to the *GOES* profile depicted in Figure 7. Here also, we clearly see the two-stage evolution of the flare in the rise phase. The overall maximum of the flare coincides at 19:19 UT, in all three energy channels. The difference of the timing in the observation of the maximum phase between hard X-ray and soft X-ray is ~ 1 minute. From the *RHESSI* measurement, the declining of the two phases is evident in the decay phase of the

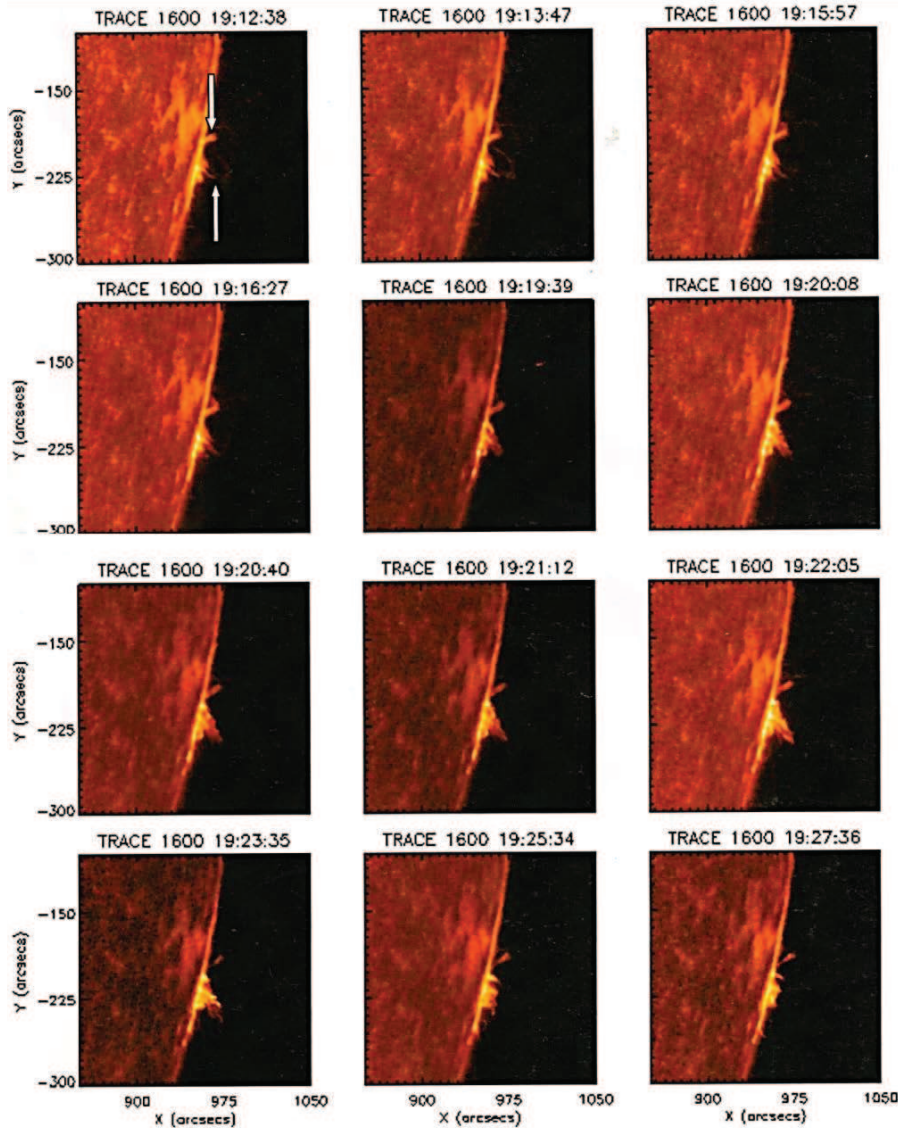


Fig. 9 Sequential *TRACE* 1600 Å images of active region 10713 during the flare. The images are recorded from the initial phase (19:12:38 UT) to the decay phase (19:27:36 UT) of the flare.

flare as well, consistent with the *GOES* findings. The decay phase begins at $\sim 19:21$ UT and at $\sim 19:26$ UT the trend changes in the light curve. The flare observations were also made by the *TRACE* satellite. *TRACE* observations for the flare were obtained in the UV range, using the filter of wavelength 1600 Å. The observation of the M1.4 class flare applying this filter is recorded from the initial phase to the decay phase. After the onset of the flare, a loop is observed in the southern part of the active region and it is the pre-flare loop. This is clearly seen from Figure 9 at 19:12:38 UT. Also, there is a small bright region observed to be present in the northern part of the active region and it could be possibly an unresolved loop structure. As the flare evolves, the pre-existing loop bright regions change, as apparent in Figure 9 at 19:13:47 UT. During the progression of the flare to the maximum phase at 19:15:57 UT,

this loop structure gets disrupted. This corresponds to the change in trend recorded in the *GOES* light curve. During the maximum phase, at $\sim 19:20:08$ UT, intense brightening is observed from both the northern and southern regions of the activity site. We find that the northern part of the active region sustains its configuration, while the southern loop system undergoes complete structural change. After 19:25:34 UT, the region does not show significant activities. This clearly indicates the second gradual stage of the decay phase during which hot plasma cools down slowly.

Emphasis is given on observations acquired by *RHESSI* on the X-ray emission originating from the coronal loops (Lin et al. 2002; Joshi et al. 2012). The *RHESSI* X-ray image (Fig. 10) for the M1.4 class limb flare is obtained at the 6–2 keV energy band. The loop top is observed at the positions $x = 957$ arcsec, $y = -218$ arc-

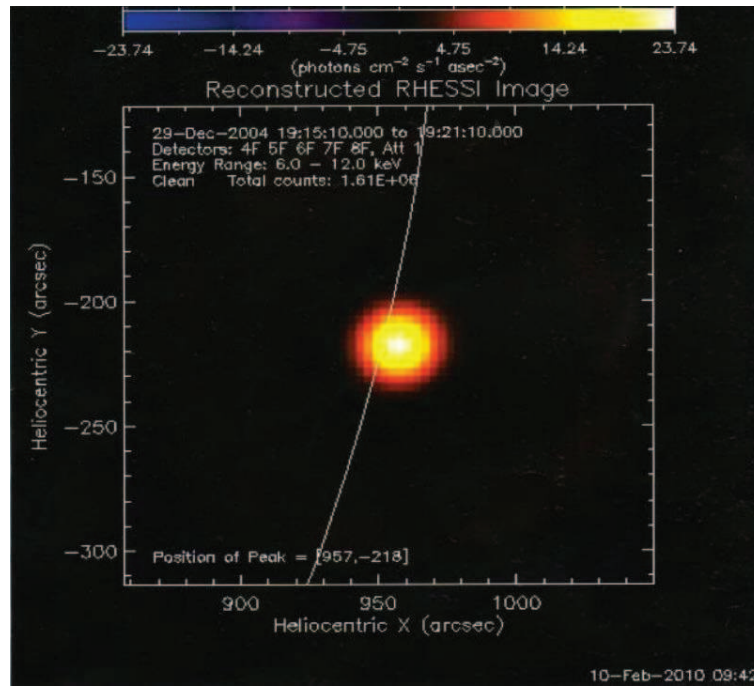


Fig. 10 Reconstructed *RHESSI* Hard X-ray image of the solar flare in the energy range 6–12 keV.

sec on the solar grid. By comparing the partial positions of *RHESSI* X-ray sources with the *TRACE* 1600 Å image, we find that X-ray emission at this energy band is originating from the coronal loops, which get disrupted during the flare. We further analyze time evolution of the 10–15 keV X-ray source during the flare from its onset to decay phase in Figure 11. We find that the X-ray source is located above the solar limb throughout the event. This suggests that the X-ray source moves upward with flare evolution, which indicates that the energy release site, which is the region of magnetic reconnection, shifts to higher altitude in the corona during the flare.

4 SUMMARY AND CONCLUSIONS

This presented work focuses on understanding the energetic processes in solar flares. We have selected two M class solar flares, one occurring close to the center of the Sun and the other close to the limb. An excellent set of multi-wavelength data enables us to understand the signature of the energy release process in different regions of the solar atmosphere in different wavelengths. A flare is a magnetic phenomenon. Data from magnetograms clearly show that flares occur in the vicinity of sunspots. These are regions of strong magnetic field with mixed polarity. Flares are accompanied by emission at different wavelengths. The flares studied in this paper provide a scenario of the energy release process in hard X-ray, soft X-ray, EUV and UV. Thus a flaring process involves all regions of the solar atmosphere. Observations of regions of brightening in

UV, EUV and also enhancement in soft X-ray flux suggest that plasma is heated to different temperatures. This provides evidence that plasma in a flaring region is multi-temperature. High energy hard X-ray emission was also observed during flares. The hard X-ray profiles are impulsive. This suggests explosive release of a huge amount of energy on a very short time scale. Theoreticians believe that such violent release of energy on short time scale can only be explained by the magnetic reconnection process. Magnetic reconnection is defined as the breaking and topological rearrangement of oppositely directed magnetic field lines in a plasma. In this process, magnetic field energy is converted to plasma, kinetic energy and thermal energy. A simple schematic diagram of the magnetic reconnection process is illustrated in Figure 12. In our analysis, we detected an X-ray coronal source in the near-limb event. This is evidentiary support for the process of magnetic reconnection in the solar corona. Due to impulsive energy release in the corona, particles (mostly electrons) are accelerated. Also the lower energy dynamics show emission in longer wavelengths of UV and EUV bands. In our flares, we find that the magnetic loop structure of the loops is observed along with the formation of new loops due to coronal energy release.

In the limb event, we found that the X-ray source moves upward in the corona, indicating that the energy release site shifts to higher altitudes. Therefore, we understand that the primary energy release during a flare takes place in the corona. These observations can be understood from the standard flare model diagrammed in Figure 13. In

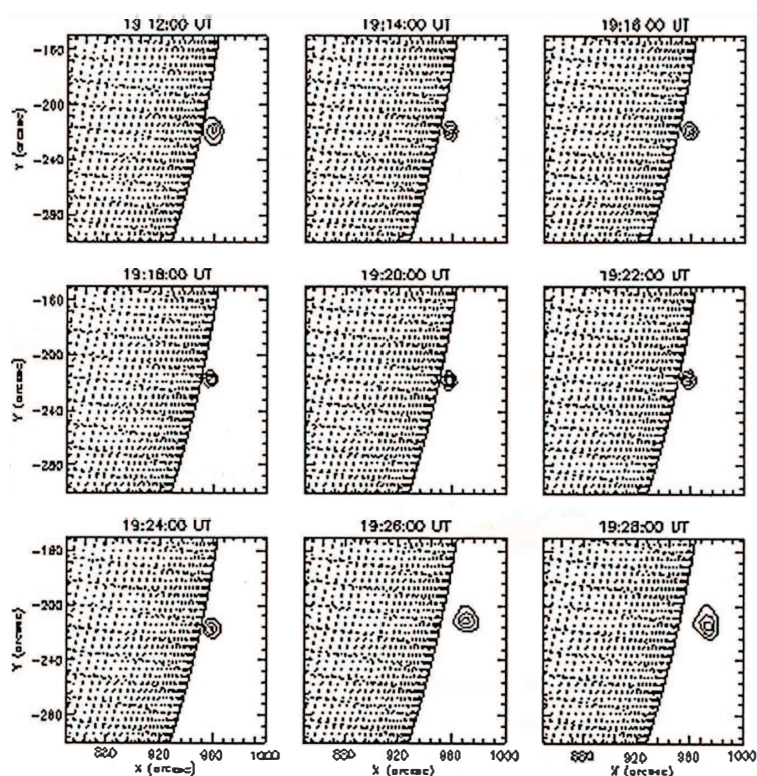


Fig. 11 Large scale contraction of coronal loops observed for 16 minutes in an M1.4 flare that occurred in active region 10713 on 2004 December 29 at location S12W90. The contraction of coronal loops can be readily seen in *TRACE* EUV images at 1600 \AA and *RHESSI* X-ray images at 10–15 keV.

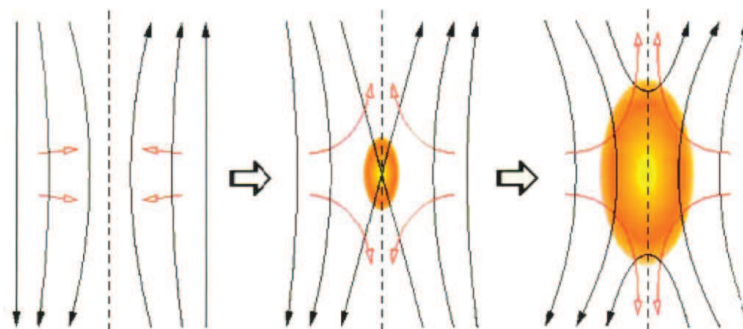


Fig. 12 Schematic representation of magnetic reconnection process.

this simplified picture, energy release takes place above the magnetic field loops that extend from the photosphere into the corona. We can see that the footpoints of the flare loops are anchored in the chromospheres, in regions of opposite magnetic polarity. Stored magnetic energy is released above the top of the loops due to magnetic reconnection. The process of energy release causes acceleration of particles (mostly electrons). The electrons are accelerated to high speed, generating impulsive hard X-ray emission. Some of the non-thermal electron are channeled down and penetrate the chromospheres at high speed, heating the plasma and thus intense brightening is observed in hard X-ray, UV and H-alpha. When beams of accelerated

protons enter the dense, lower atmosphere, they may produce nuclear reactions resulting in gamma rays in some exceptionally energetic flares. Materials in the chromosphere are heated quickly and rise into the loops which result in a slow gradual increase in soft X-ray radiation.

In the disk event presented in this paper, we clearly observed brightening of the lower and denser atmospheric layers, which is the chromospheric and transition region, in the form of ribbon-like structures in UV images. From the above study, we can conclude that the multi-wavelength and multi-instrumental analysis has improved our understanding of various physical processes during a solar flare occurring in different layers of the solar atmosphere. The s-

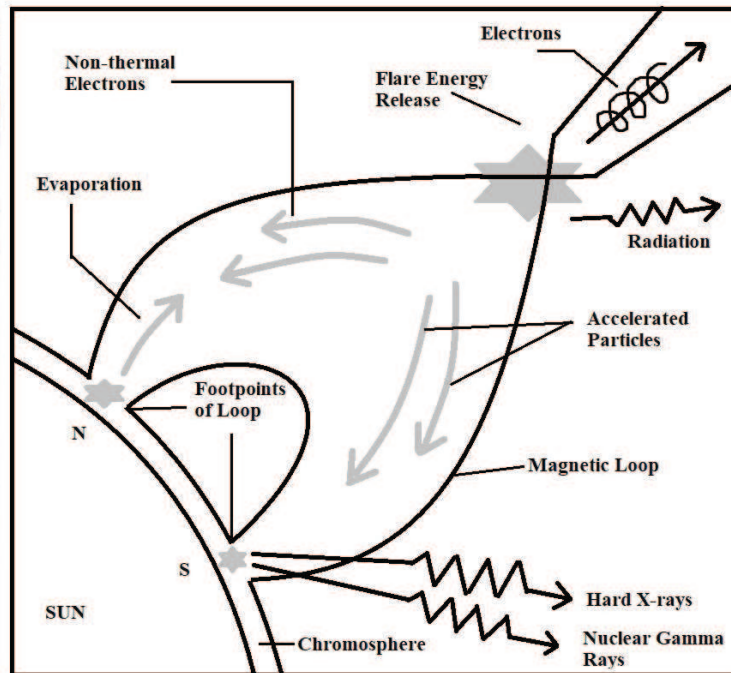


Fig. 13 Standard flare Model.

tandard flare models broadly recognize these physical processes as the consequence of large scale reconnection of magnetic field lines in the corona. However, advancements in the observational capabilities of modern equipment have led to several new insights into the flare evolution that deviate from standard models. Flares have been observed for more than 150 years and many investigators studied them during the last three to four decades, but still we are far away from a full understanding of the evolution of flares. We have yet to comprehend various basic elements causing pre-flare magnetic configuration, energy release process and site, triggering mechanism, conversion of magnetic energy to heat and kinetic energy, particle acceleration, etc. These unsolved issues pose challenges for future researchers.

Acknowledgements The authors are grateful to the CME catalog from *SOHO/LASCO* observations maintained and generated by the CDAW Data Center, NASA. We thank Prof. Bhuwan Joshi, USO, Physical Research Laboratory, Ahmedabad, and Prof. Hari Om Vats, scientist, Physical Research Laboratory, Ahmedabad, India for their great support to us. Thanks are also due to an anonymous referee for helpful suggestions. I am thankful to the Madhya Pradesh Council of Science and Technology for providing me funding under the FTYS program for the training at KSKGRL, Indian Institute of Geomagnetism, Allahabad,

India.

References

- Abramenko, V. I., Gopasyuk, S. I., & Ogir', M. B. 1991, *Sol. Phys.*, 134, 287
- Cui, Y., Li, R., Zhang, L., et al. 2006, *Sol. Phys.*, 237, 45
- Deng, Y.-Y., Wang, J.-X., Yan, Y.-H., & Zhang, J. 2001, *Sol. Phys.*, 204, 13
- Hagyard, M. J. 1990, *Mem. Soc. Astron. Italiana*, 61, 337
- Hagyard, M. J., Moore, R. L., & Emslie, A. G. 1984, *Advances in Space Research*, 4, 71
- Hirayama, T. 1974, *Sol. Phys.*, 34, 323
- Joshi, B., Veronig, A. M., Lee, J., et al. 2011, *AJ*, 743, 195
- Joshi, B., Veronig, A., Manoharan, P. K., & Somov, B. V. 2012, *Astrophysics and Space Science Proceedings*, 33, (Berlin Heidelberg: Springer-Verlag), 29
- Kopp, R. A., & Pneuman, G. W. 1976, *Sol. Phys.*, 50, 85
- Kumar, P., Srivastava, A. K., Filippov, B., et al. 2011, *Sol. Phys.*, 272, 301
- Lin, R. P., Dennis, B. R., Hurford, G. J., et al. 2002, *Sol. Phys.*, 210, 3
- Moon, Y.-J., Choe, G. S., Yun, H. S., et al. 2002, *ApJ*, 568, 422
- Pevtsov, A. A., Fisher, G. H., Acton, L. W., Longcope, D. W., et al. 2003, *ApJ*, 598, 1387
- Priest, E. R., & Forbes, T. G. 2002, *A&A Rev.*, 10, 313
- Sturrock, P. A. 1996, *Nature*, 211, 695
- Wang, T.-J., Sui, L.-H., & Qiu, J. 2007, *ApJ*, 661, L207